Characterization of Geoobjects Continuity using Moments of Inertia

Saina Lajevardi, Olena Babak, and Clayton V. Deutsch

Well-placement is one of the main challenges in reservoir engineering. The connectivity of the net reservoir is often modeled by geostatistical tools so that the most efficient part of the reservoir in terms of fluid flow and petrophysical features (e.g. porosity and permeability) can be located. In the study of well placement, non-net barriers are to be avoided for efficient fluid flow. Barriers which obstruct oil flow must be identified and avoided during recovery. In this work, the connectivity of the non-net barrier (the undesirable components) is studied; this is in contrast to the usual focus on the net continuity of the reservoir. A sound understanding of non-net barriers, in terms of their orientation, size and "tortuosity" could help with effective well placement when no reservoir modeling is provided. In this study, tortuosity is defined as the normalized area that is in excess of a fitted ellipsoid of the same volume; it is used here as a measure of "shape irregularity." Our results show that there is no correlation between a barrier's tortuosity and its size, which explains why tortuosity is required to be characterized as an individual property of the barrier.

Introduction

This study focuses on "good" reservoirs, where the shales (i.e. barriers) occupies less than $25-30\%$ of the total reservoir volume, see Fig. 1. These barriers, which are assumed to be in the form of unconnected pockets form the non-net components of the geological formation. This is in contrast to the traditional approach where the focus is on the connectivity of sand (i.e. net components) in the reservoir. The concept of characterizing the barriers, which exist as unconnected "pockets" within the formation, is the unique feature of the present study.

In [1], the authors had focussed on characterizing the continuity of objects according to their thicknesses and areal extensions. Mass moments of inertia were used for calculating the size, geometry, and orientation of the objects. Details of this analysis will be discussed later. Their results showed that there was correlation between the areal extension and the thickness of the objects. Here, we postulate that knowledge of only the sizes of the objects is not sufficient for characterizing reservoir connectivity; effective well placement will require also knowledge of how "irregular" each object is, as irregular shapes lead to decrease in overall effective permeability and flow impedance. In this paper, we will introduce a "tortuosity" parameter as a measure of shape irregularity. This tortuosity is derived using a mass moment of inertia analysis similar to that of [1]. In what follows, we will first outline the methodology for obtaining such a tortuosity parameter. We will then demonstrate that there is no clear correlation between tortuosity (i.e. shape irregularity) and the object size.
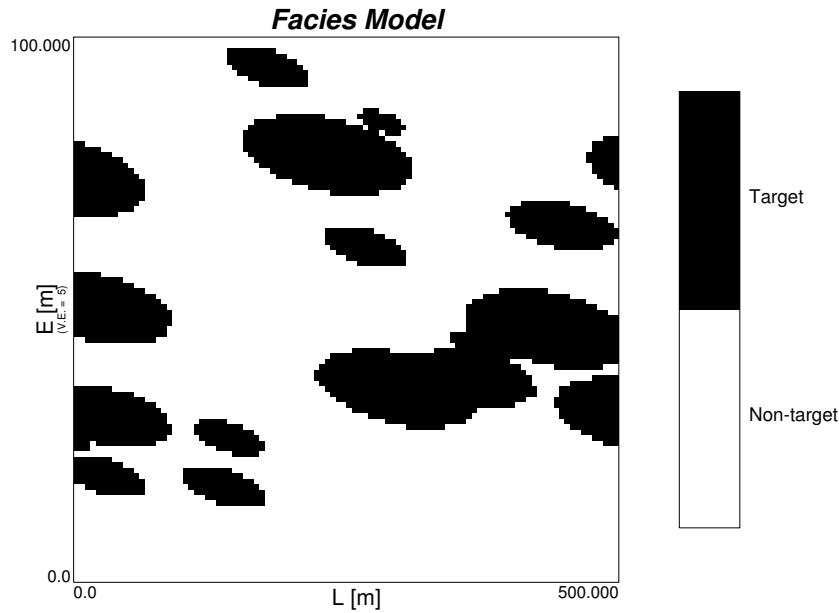
Figure 1: Reservoir model example with 20% non-net barrier.

Methodology

The initial concept is to reconsider every barrier (non-net component) as an object and represent it as an ellipsoid which has the same size and orientation as the object. Recognizing that irregular objects invariably have larger surface areas, we focus especially on the calculation of the surface area, given that the objects and ellipsoids were "coarse grained" into cubical grid cells. These calculations lead to the definition of a ratio which could be considered an estimate of the tortuosity of an object. This knowledge could be applied, for example, as an alternative to 3D modelling for SAGD well placement.

Object size determination is carried out by equating the moments of inertia of the object to that of a perfect ellipsoid. The inertia tensor (I) for the ellipsoid is diagonal if the ellipsoid's principal radii are aligned with the Cartesian axes (rotated in general). The key to this analysis is to keep the volume of the ellipsoid the same as that of the object. This is achieved by first calculating the object's mass moment of inertia $I = \sum_{i=1}^{N} m_i \, r_i^2$. The object is then approximated as an ellipsoid by matching the moments of inertia of the two entities. What results from this calculation is the set of principal radii of the equivalent ellipsoid, which in general would have a volume slightly different from that of the object. Finally, to ensure that the object and the ellipsoid have the same volume, the three principal radii are rescaled by a common factor (determined by the mismatch in volume).

Mass Moments of Inertia

As explained earlier, the principal axes for each object are determined based on the ellipsoid approximation [1]. The ellipsoid's center is adjusted to coincide with the object's center of

mass, which can be calculated from the *first* moments of inertia:

$$\overline{x} = \frac{\sum_{i=1}^{N} m_i x_i}{\sum_{i=1}^{N} m_i} \quad ; \quad \overline{y} = \frac{\sum_{i=1}^{N} m_i y_i}{\sum_{i=1}^{N} m_i} \quad ; \quad \overline{z} = \frac{\sum_{i=1}^{N} m_i z_i}{\sum_{i=1}^{N} m_i} \quad ;$$

where the m_i's represent discretized masses (N is the total number of cells). To determine the ellipsoid's principal axes, the *second* moments of inertia should be calculated. Unlike the first moment, which is a vector, the second moment I is a tensor given by

$$I = \begin{bmatrix} I_{xx} & I_{xy} & I_{xz} \\ I_{yx} & I_{yy} & I_{yz} \\ I_{zx} & I_{zy} & I_{zz} \end{bmatrix}$$

where

$$I_{xx} = \sum_{i=1}^{N} m_i \ (y_i{}^2 + z_i{}^2); \qquad\qquad I_{xy} = I_{yx} = -\sum_{i=1}^{N} m_i \ x_i \ y_i$$

$$I_{yy} = \sum_{i=1}^{N} m_i \ (x_i{}^2 + z_i{}^2); \qquad\qquad I_{xz} = I_{zx} = -\sum_{i=1}^{N} m_i \ x_i \ z_i$$

$$I_{zz} = \sum_{i=1}^{N} m_i \ (x_i{}^2 + y_i{}^2); \qquad\qquad I_{yz} = I_{zy} = -\sum_{i=1}^{N} m_i \ y_i \ z_i.$$

Note that the matrix I is symmetric by definition. This means that its eigenvalues are all real, and its eigenvectors are orthogonal to one another. We will let the three eigenvalues be (I_1, I_2, I_3). Now, if the object is a perfect ellipsoid with principal radii (r_a, r_b, r_c), its principal moments of inertia would be

$$I_a = \frac{1}{5} \ M \ (r_b{}^2 + r_c{}^2)$$

$$I_b = \frac{1}{5} \ M \ (r_a{}^2 + r_c{}^2)$$

$$I_c = \frac{1}{5} \ M \ (r_a{}^2 + r_b{}^2)$$

where M is the total mass of the ellipsoid. To approximate the object as an ellipsoid, we now equate (I_1, I_2, I_3) to (I_a, I_b, I_c). This way, the principal radii (r_a, r_b, r_c) will be expressed in terms of (I_1, I_2, I_3) and can therefore be evaluated numerically. In the exact calculation M should be considered as the volume of the ellipsoid, which is given by $V = \frac{4\pi}{3} \ r_a r_b r_c$. This leads to set of non-linear equations which could be solved numerically.

Determination of surface area is not as accurate since the objects are made of discretized cells. In this study, we deliberately discretized the ellipsoid in the same way the object is discretized. This way, the two surface areas can be compared on a common basis (in particular, errors which result from discretization will hopefully cancel when calculating
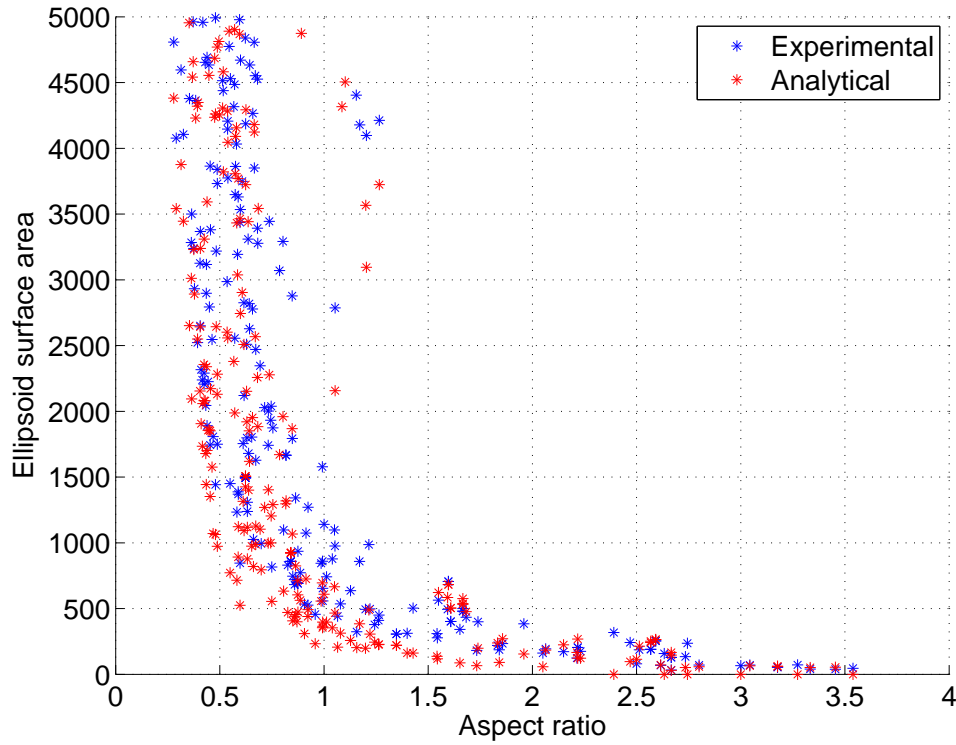
Figure 2: Fitted ellipsoid SA vs aspect ratio.

the *difference* between the surface areas). In general, every object is made of interior and exterior cells. Cells whose all six neighbors are non-net (density 1) are identified as interior cells and will be ignored in surface area calculation. On the other hand, cells with at least one net neighbor (density 0) will be recognized as the exterior cells. Every exterior cell will be counted from 1 to 5 based on the number of sides that are outward-facing. This can result in significant errors due to discretization (e.g. approximating a tilted surface as a series of right-angle steps). However, subtraction of two surface areas (both carrying discretization errors) could hopefully result in cancelation of such errors.

In the discretized context, evaluation of surface area is equivalent to adding up the number of exposed faces of the exterior cells. The interior cells could be recognized by the non-net neighbours while the outer cells would have at least have one face exposed to a net cell neighbor. This way, the error due to discretization would stay same for both approximations. Of course, the size and surface area of the fitted ellipsoid could be theoretically evaluated as follows:

$$V_{\text{ellipsoid}} = \frac{4\pi}{3} r_a r_b r_c,$$

$$A_{\text{ellipsoid}} = 4\pi \left(\frac{(r_a \times r_b)^\rho + (r_a \times r_c)^\rho + (r_b \times r_c)^\rho}{3} \right)^{1/\rho}.$$

As Fig. 2 demonstrates the analytical surface area for the fitted ellipsoid deviates from that of the experimental (counting) one. This deviation is due to discretization approach and should be considered in the analysis approach. In the following section, we discuss our methodology to quantify the objects' irregularity.

Analysis and Discussions

We use training image library in GSLIB to experiment the object's characterization for numerus models. Also, we have generated some reservoir models using ELLIPSIM program based on the percentage of net and non-net components (see Fig. 1). The size of the model could be arbitrary and the non-net components in this study should not fill more than 30% of the reservoir volume. A modified program extracted from GEO-OBJ [2] program is also used to identify the objects in the model. After the objects are identified, a program called TORTUOSITY, which has been developed during this study, is used to evaluate the size, orientation and tortuosity of the objects.

As was mentioned earlier, an object's geometrical properties are characterized by its moments of inertia. The mass of every cell is assumed to concentrate at the center of the cell. As one radius of the object approaches the cell dimension, the eigenvalues of the tensor begin showing erratic behaviors and should be avoided during the computations. In many cases, one or more of the principal radii approaches zero. Also, there are barriers which are distributed mostly on the lateral extension and resemble planar shapes. Such sheet-like objects could be identified using eigenvectors. By first arranging the eigenvalues in ascending order such that $I_a < I_b < I_c$ we expect the following characteristic for a sheet-like object:

$$\frac{I_a + I_b}{I_c} \approx 1,$$

According to above relationship, using TORTUOSITY program such barriers could be identified and later be recognized by that extra characteristics.

Tortuosity

One important property of the barriers which help characterize the continuity of the non-net reservoir is how irregular the shapes of the barriers are. It is clear that, for a given volume, the more irregular the shape, the larger would be its surface area. Based on this idea, we define the "tortuosity" T as the surface area of the object that is in excess of an ellipsoid of the same volume. (We chose not to compare the surface area to an equal-volume sphere (which has the least surface area for a specific volume), as spherical shapes are too far removed from the overall orientation of the real object.) This excess area is non-dimensionalized by dividing it by the area of the ellipsoid as follows:

$$T = \frac{A_{object} - A_{ellipsoid}}{A_{ellipsoid}}.$$

Note that a value of $T = 0$ represents a non-tortuous shape, while a large T value suggests that the barrier is very tortuous. In principle, our defined tortuosity factor should not be less than zero (Surface area of object is always greater than the surface area of the same-size fitted ellipsoid). However, for some objects the value of T tends to be a small negative number which results from numerical noise due to discretization. This happens more as the size of the object gets much more comparable to the unit cubic cell.

As mentioned before, a GSLIB program called TORTUOSITY has been developed in order to study how irregular every object is located in the reservoir. In this study, the ellipsoid represents every object's volume and orientation. The eigenvectors calculated from the moment of inertia tensor of every object are used to locate and tilt the ellipsoid (of equivalent volume). In this approach, both the object and the ellipsoid will be discretized. The size determination and surface area approximation for both will be evaluated numerically rather than analytically. The output files of this program provides information regarding the object's size, ellipsoid size, thickness of the object, areal extension, surface area, aspect ratio and tortuosity factor for every object.

Table 1: Tortuosity factor for similar-size objects.

Object No.	Object Size (V)	Tortuosity Factor (T)	Aspect Ratio
1	17215	0.0452	1.4671
2	17754	0.7668	4.8439
3	17795	1.0527	8.624
4	1552	0.0138	2.0896
5	1584	0.5807	4.5183
6	1140	1.0070	5.9402

The orientation of the ellipsoid is specified by the direction of its principal axes, which are in turn given by the eigenvectors of the moment of inertial tensor. The output file of TORTUOS program lists the tortuosity factor for every object available in the model which has a volume size greater than 10 units. (Very small objects, because of discretization issues, will lead to computational difficulties. This, however, should not be a concern as we are more interested in larger objects.)

In this study, every face which is exposed to the net region contributes equally to the surface area of the ellipsoid and the object. Basically, every cell could contribute between 1 and 5 faces to the surface area, depending on how sharp the local curvature is. If the ratio of surface area to volume reaches 6, it is a sign that the size of the object is approaching the cell size, which leads to less exact calculations and harder understanding of the objects. The validity of tortuosity definition could be for example demonstrated in Fig 6; the last object in this figure corresponds to a high T value. However, the fist object in the same figure represents lower tortuosity and smoother surface.

It is also of interest to look for possible correlations between tortuosity and the object size. Fig. 3 represents the correlation of the tortuosity factor T and the size of the object. For the smaller objects, the ratio is sitting closer to 0.0. This is expected since for the smaller objects, there is not much room for surface area deviation. However, this

deviation is more obvious for bigger objects as they have naturally bigger surface area and consequently more chances for tortuosity. A possible reason could be, during the formation of the barriers (over geological time scales), the bigger objects may be the ones that take on more irregular shapes. However, as seen in Fig. 3, there appears to be no correlation between T and the object size. (Note that the data corresponding to small objects, e.g. with sizes less than a few hundreds, are not reliable due to discretization errors.)

Experimental Results

Fig. 4 represents the distribution of the object's size, tortuosity and aspect ratio which have been experimented in this study. There is no clear correlation between these features. Also, as can be seen from Fig. 3, no correlation can be captured; this explains the importance of understanding of barrier regardless its size and orientation. Table 1 lists some objects with their properties; see Fig. 5 for objects 1, 2, 3 and 6 for objects 4, 5, 6. Objects with same size have been compared in terms of their tortuosity. The listed objects are visualized in figures 5, 6. The visualized objects validate the correctness and effective description of tortuosity factor. The tortuosity is calculated and visualized to be independent of the object's size which is an important feature for further analysis.

As explained earlier, baffles with small tortuosity are of less impedance to oil recovery. Another interesting observation is to consider a very big object with tortuosity factor less than 0.1; see Fig. 7. This reinforces our suspicion that there is no clear correlation between tortuosity and size (i.e. tortuosity does not increase monotonically with size).

Conclusions

This study proposes an approach to quantify the tortuosity of the barriers in addition to the determination of the size and orientation of the object. Characterizing the objects' properties contributes to understanding the connectivity of the non-net reservoir, which is of main interest to reservoir modeling. Apart from the size and orientation of the object, which should be determined for well-placement and further application, how tortuous the barrier is also plays an important role in recognizing the effectiveness of well-placement. This has not been studied before and cannot be determined by evaluation of only the size and orientation of the objects. The key result of this study is the fact that size evaluation alone cannot account for the tortuosity of the barriers; a sound understanding of how the surface of the object deviates from that of a "well-behaved" ellipsoid could result in different reservoir decisions and actions. The simulation results showed that the objects with the same size could have different tortuosity properties. This will lead to different affect on fluid flow for oil recovery.

References

[1] O. Babak and C. V. Deutsch, "Nonnet size determination with mass moments of inertia," *CCG Report*, no. 10, pp. 132–1,132–6, sept 2008.

[2] C. V. Deutsch and A. G. Journel, *Geostatistical Software Library and User's Guide*, 2nd ed. Oxford University Press, New York, 1998.
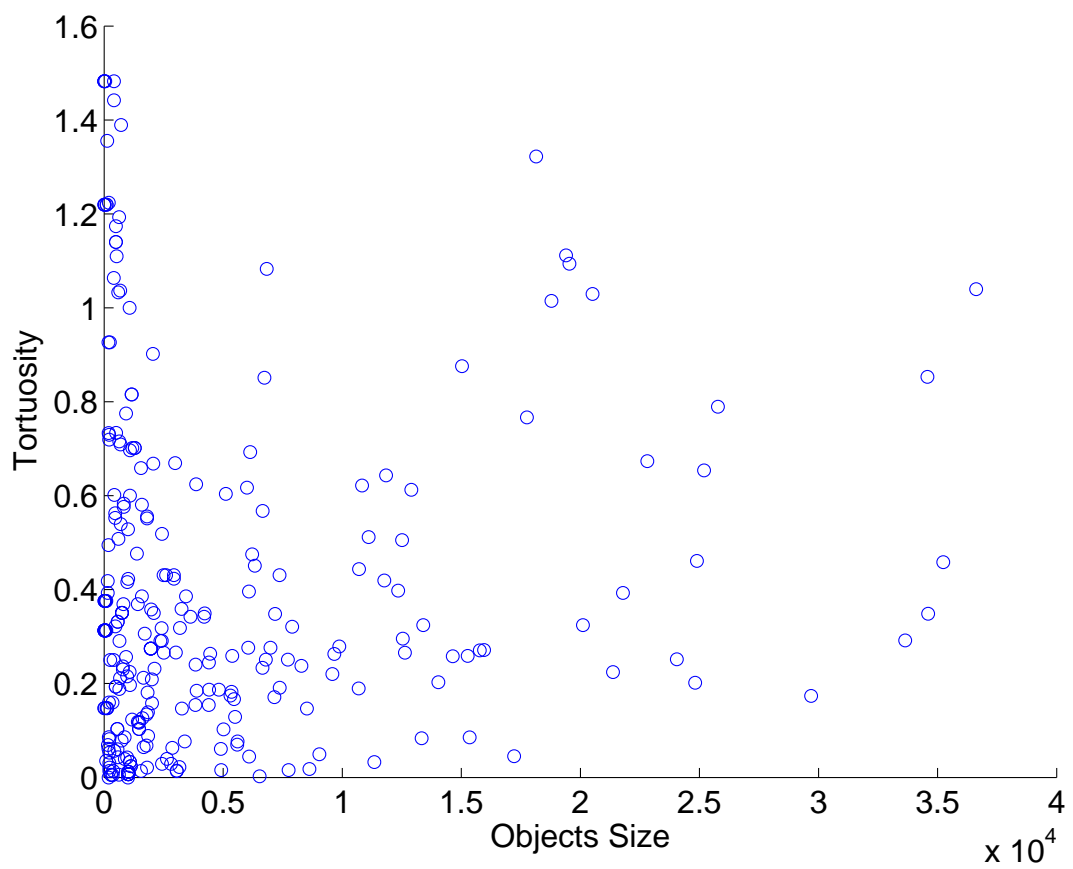
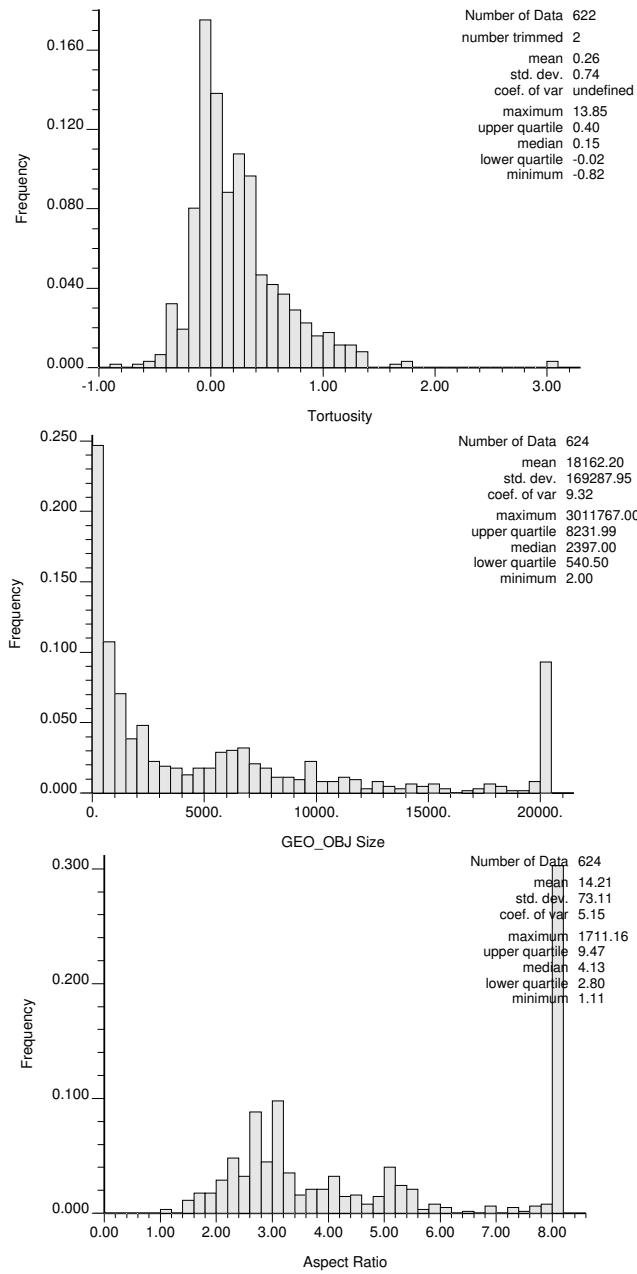**Figure 3:** Tortuosity versus object's size for about 400 objects.

Figure 4: The distribution of tortuosity, object's size and aspect ratio from top to bottom.
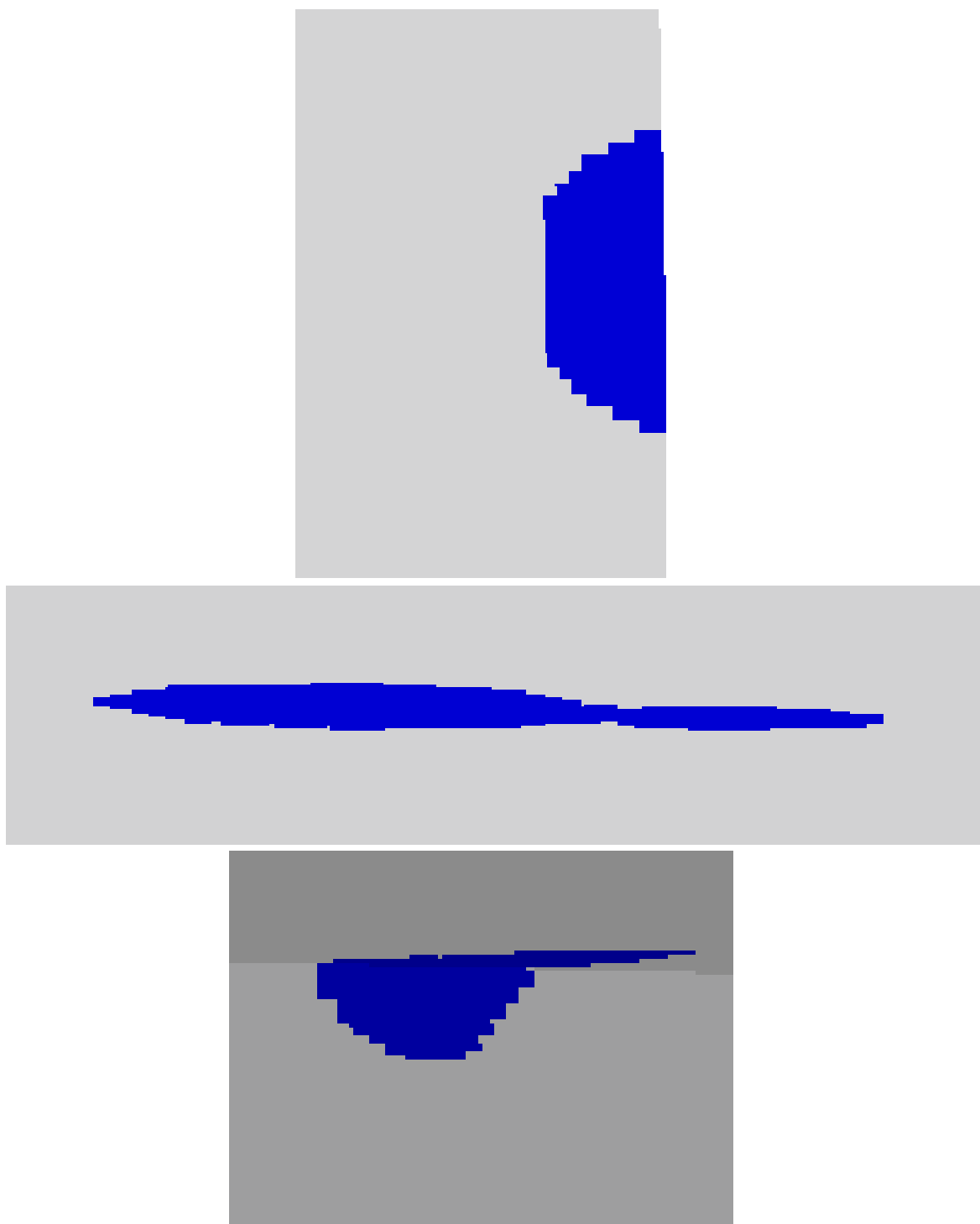
Figure 5: Smaller objects with different tortousity (from above1,2,3 in table 1)
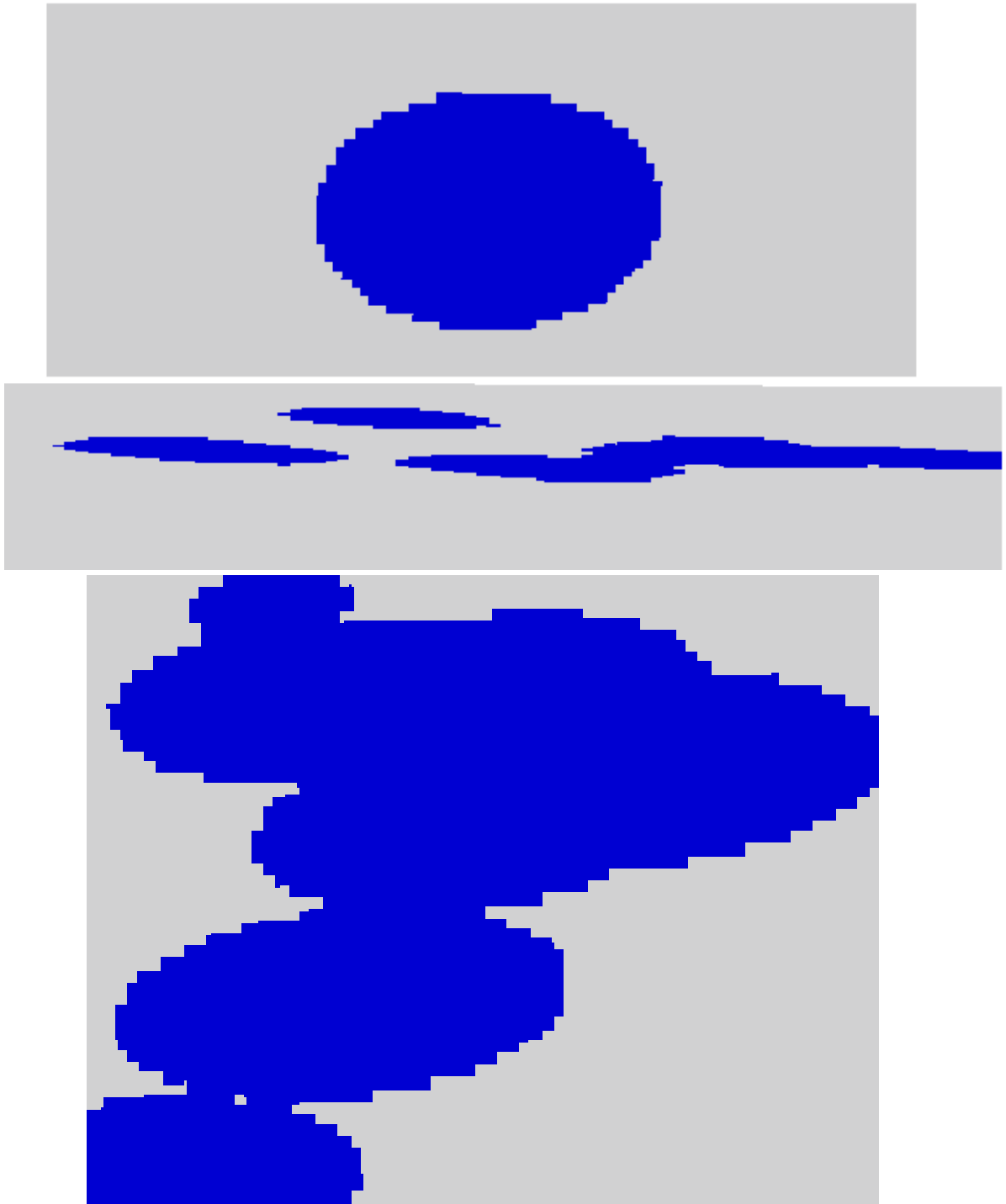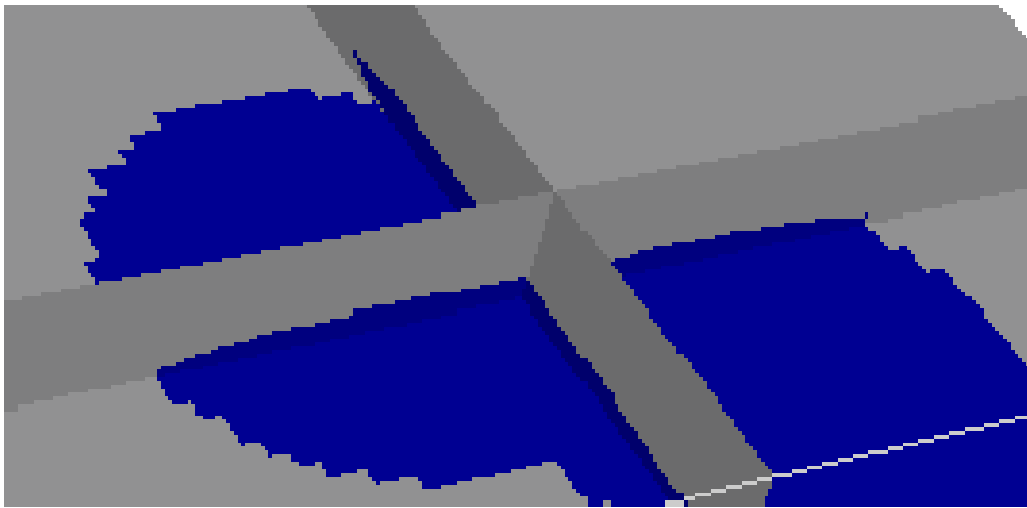
Figure 6: Objects 4, 5 and 6 in table 1.

Figure 7: Big object with small tortuosity (less than 0.1).